

# Relations between cold drawing behaviour and optomechanical properties of vestan (polyester) fibres

I. M. FOU DA, M. M. EL-TON SY

*Physics Department, Faculty of Science, Mansoura University, Mansoura, Egypt*

A modified stress-strain device is used to investigate the dynamical behaviour of optomechanical properties. The optical properties and strain produced in vestan fibres by different stresses have been measured at room temperature interferometrically. It has been found that the relation between strain and birefringence is linear up to strain of 12%. For greater strain the rate of change of birefringence with strain is cut off due to breaking. An empirical formula is suggested to represent the variation of the cross-sectional area of vestan fibres with draw ratio and the constants of this formula are determined. An expression has also been suggested for the birefringence related to the strain. The strain optical coefficient is determined. Poisson's ratio, Young's modulus, elastic shear modulus and the compressibility are calculated over different strain values. Microinterferograms are given for illustration.

## 1. Introduction

An isotropic polymer has the same structure and properties in all directions. Upon deformation in the solid state, the polymer becomes anisotropic because the polymer chains align and therefore become oriented with respect to a particular direction. The degree of orientation with respect to a particular direction expresses a measure of the extent of anisotropy produced by the deformation process. Since the properties of an anisotropic polymer show a directional dependence, a measurement of the orientation in the polymer portrays how its properties are modified during deformation. Orientation in a polymer can be detected by a number of different techniques. Depending on its constitution, the results from optical techniques can be used to obtain information about the orientation of the fibrous materials [1].

A synthetic fibre spun from the melt of a certain polymer by extrusion through fine holes has almost no desirable textile properties and a low birefringence. In order to turn it into a useful textile fibre it must be mechanically drawn out to make it thinner, stronger and consequently more birefringent. Orientation can be obtained by mechanical drawing and is often accompanied by a change in structural characteristics. Birefringence gives a measure of orientation which is an average of the amorphous and crystalline regions [2]. Interferometric methods offer a highly accurate determination of the indices of refraction and birefringence of natural and synthetic fibres [3-7].

Optical anisotropy produced in fibres by stretching gives valuable information for characterization of these fibres on the molecular level. An analysis of the relation between the birefringence and the draw ratio of some synthetic fibres has been given [8-15].

In the present work, a microstrain device, used

previously [15], was modified to study the change of the refractive indices, the birefringence and strain was produced in vestan (polyester) fibre by different stresses at room temperature. The relationship between the birefringence and the mechanical parameters has been found. The data obtained were utilized to calculate the polarizability per unit volume. An attempt has also been made to explain the strain-birefringence curves.

## 2. Experimental details

### 2.1. Design of apparatus used to measure stress-birefringence

The modified form of the device is shown in Fig. 1. A small spring balance B provided with four wheels h1, h2, h3 and h4 has been introduced to the strain device previously designed [15], in such a way that the four wheels are running on the smooth cylindrical rods bd and b'd'. The body of the balance is fixed on the sliding bar c, while an end of the fibre is fixed to the second terminal of the balance (the free end of the balance's spring). The other end of the fibre is tightly fixed to the edge of the optical flat F, which is fixed horizontally in the metallic jig J. To determine the initial fibre length  $l$ , the fibre is fully straightened and measured by a vernier scale. When the threaded rod e is pulled out (screwed out) the balance is moved away from jig J and hence the fibre is stretched by the spring of the balance. A fine pointer P reads the net elongation,  $\Delta l$ , produced on the metric scale S, while the balance shows the actual mass,  $m$ , needed to stretch the fibre. The frame may then be transferred to the microscope stage. Another 70% silvered optical flat is fitted in the jig to form a wedge interferometer for producing multiple-beam Fizeau fringes in transmission as discussed elsewhere [3-5].

In the present work, the mean refractive index  $n_a^{\parallel}$  of

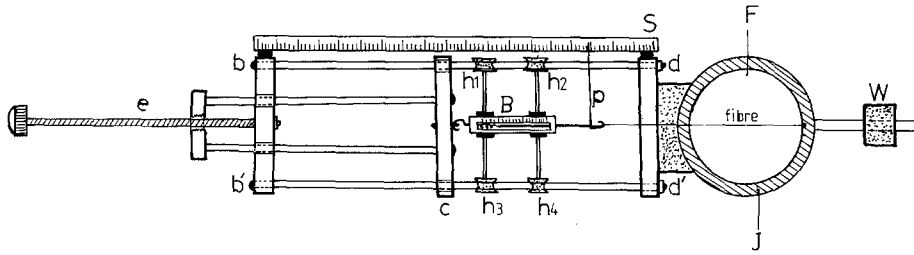


Figure 1 Schematic diagram of the modified stress-strain device.

the fibre for monochromatic light, of wavelength  $\lambda$ , vibrating parallel to the fibre axis will be calculated by the following relation [5]

$$n_a^{\parallel} = n_L + \frac{dz^{\parallel} \lambda}{2t_f h} \quad (1)$$

with an analogous formula for  $n_a^{\perp}$ , where  $n_L$  is the refractive index of the immersion liquid,  $dz$  the shift size,  $t_f$  the fibre thickness and  $h$  the interfringe spacing.

The experimental values of the mean polarizabilities per unit volume parallel,  $P_a^{\parallel}$ , and perpendicular,  $P_a^{\perp}$ , to the axis of stretching fibre were obtained from the measured values of the mean refractive indices  $n_a^{\parallel}$  and  $n_a^{\perp}$  for plane polarized light vibrating parallel and perpendicular to the fibre axis, respectively. The calculation was done using the Lorentz-Lorenz equation

$$\begin{aligned} P^{\parallel} &= 3(n_{\parallel}^2 - 1)/4(n_{\parallel}^2 + 2)\pi \\ P^{\perp} &= 3(n_{\perp}^2 - 1)/4(n_{\perp}^2 + 2)\pi \end{aligned} \quad (2)$$

The experimental values of Young's modulus,  $E$ , of the fibre material were measured for each draw ratio of the fibre by recording the stress and the corresponding strain several times until the cut-off stress for the fibre, the formula used for calculating  $E$  [16] is

$$E = \frac{F/A}{\Delta l/l} \quad (3)$$

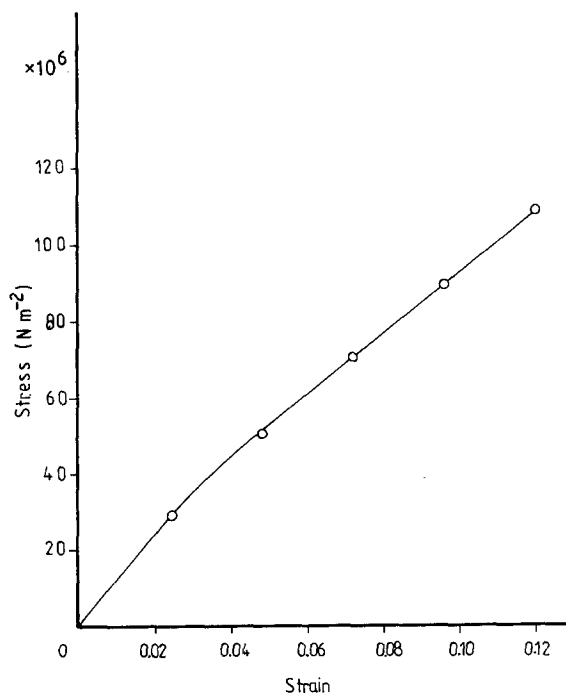


Figure 2 Stress-strain behaviour of vestan fibre at a temperature of 33.5°C.

where  $F$  is the force acting along the axis of the fibre,  $A$  the cross-sectional area of the fibre,  $l$  the initial length and  $\Delta l$  is the produced elongation.

Fig. 2 shows the stress-strain behaviour of vestan (polyester) fibres measured by the developed micro stress-strain device (Fig. 1). It is clear that vestan fibres obey Hook's law only in a very small range of

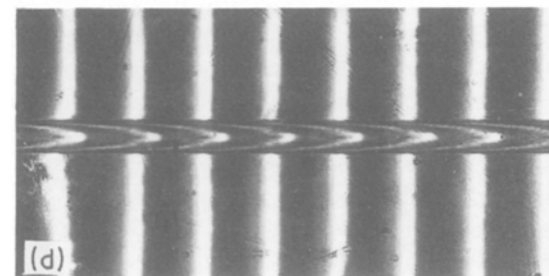
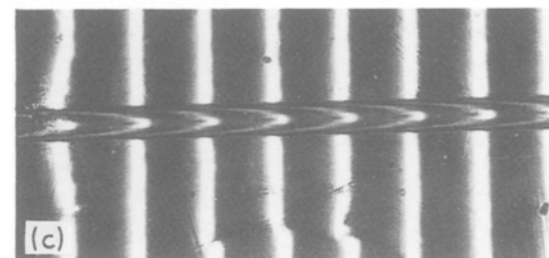
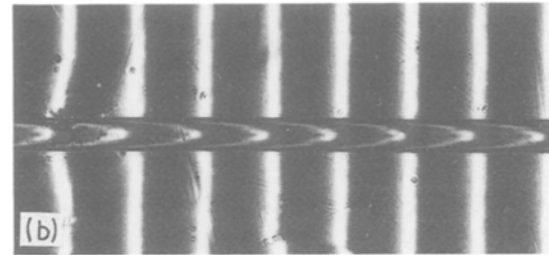
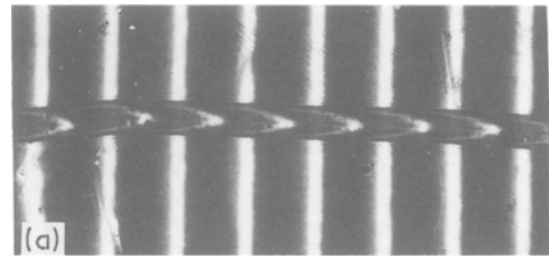


Figure 3 Microinterferograms of multiple-beam Fizeau fringes in transmission for vestan fibre using light vibrates parallel to the fibre axis (draw ratios (a) 1.000, (b) 1.048, (c) 1.096 and (d) 1.120).

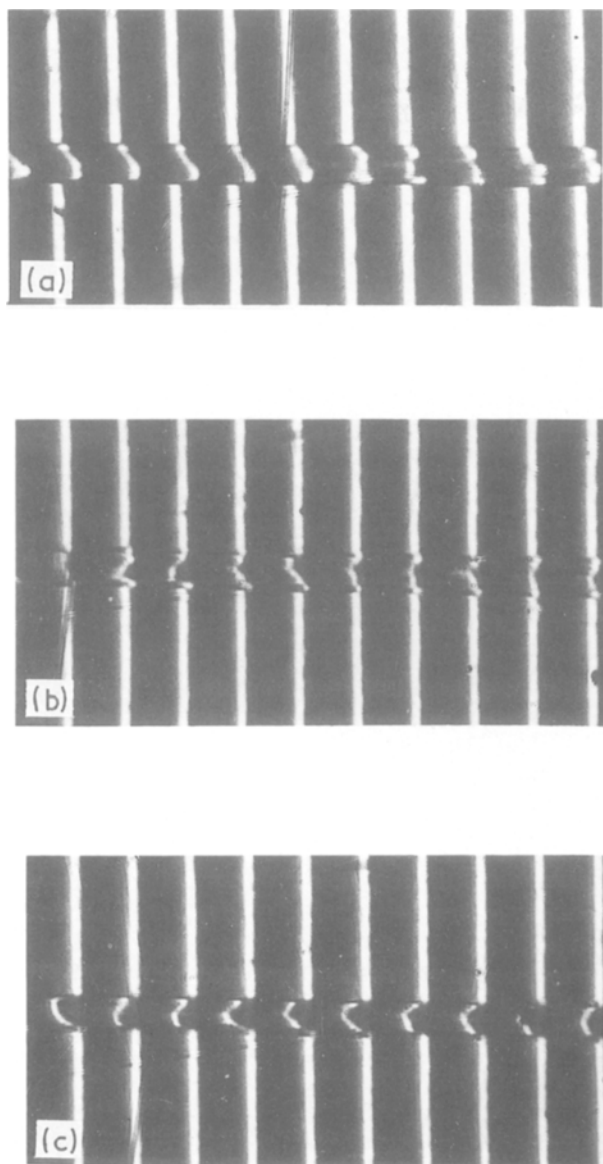


Figure 4 Microinterferograms of multiple-beam Fizeau fringes in transmission using light vibrates perpendicular to the fibre axis (draw ratios, (a) 1.021, (b) 1.043 and (c) 1.064).

the applied stress. This may be due to relatively high birefringence for vestan fibres.

Figs 3a, b, c and d are microinterferograms of multiple beam Fizeau fringes in transmission for vestan fibre. Plane polarized light of wavelength  $\lambda = 0.5461 \mu\text{m}$  vibrating parallel to the fibre axis is used at fibre draw ratios of 1.000, 1.048, 1.096 and 1.120, respectively. The refractive index of the used immersion liquid was  $1.6286 \pm 0.0002$  at a temperature of  $33.5^\circ\text{C}$ . Figs 4a, b and c are microinterferograms for another sample of vestan fibre for the multiple-beam Fizeau fringes in transmission. Plane polarized light of wavelength  $\lambda = 0.5461 \mu\text{m}$  vibrating perpendicular to the fibre axis is used at draw ratios 1.021, 1.043 and 1.064, respectively. The refractive index of the used immersion liquid in this direction was  $n_L = 1.5359 \pm 0.0002$  at a temperature of  $33.5^\circ\text{C}$ . The use of two different samples and two different immersion liquids was essential with vestan fibres due to the relatively high birefringence of the

material. It is clear from Figs 3 and 4 that the change in fringe shifts is obtained by increasing the applied stress at different draw ratios.

The changes of fibre radius and hence cross-section area could not be observed clearly, by increasing the applied stress, from the obtained microinterferograms. To calculate these changes we can assume that the volume is constant by loading the sample. Hence, the change  $\Delta A$  of the cross-section area may be calculated from the relation

$$\Delta A = (A\Delta l)/(l + \Delta l) \quad (4)$$

where  $A$ ,  $l$  and  $\Delta l$  are as previously defined. As a special case, for fibres of very small radius contraction by loading, and on the base of the assumption of constant volume, the radius contraction  $\Delta r$  may be calculated from the approximate formula

$$\Delta r = (r\Delta l)/2(l + \Delta l) \quad (5)$$

where  $r$  is the radius of the unloaded fibre. Introducing the value of  $\Delta r$  given in Equation 5 into the well known definition of Poisson's ratio [15]  $\mu$ , for fibres of very small radius contraction, we obtain

$$\mu = -\frac{\Delta r/r}{\Delta l/l} = \frac{l}{2(l + \Delta l)} = \frac{1}{2R} \quad (6)$$

where  $R = (l + \Delta l)/l$  is the draw ratio.

Table I gives the experimental values of Poisson's ratio of vestan fibre at different draw ratios. The same table shows the change of fibre cross-sectional areas,  $A$ , by changing the draw ratio  $R$ . It was found that  $A$  varies with  $R$  according to the empirical relation

$$A = \alpha R^{-\beta} \quad (7)$$

where  $\alpha$  and  $\beta$  are constants that characterize the deformation process. A plot of  $\ln A$  against  $\ln R$  gives values of  $\alpha$  and  $\beta$ . For vestan fibres values of  $\alpha = 1.363 \times 10^3 \mu\text{m}^2$  and  $\beta = 1.025$  were found.

Fig. 5 shows the change of fibre cross-sectional area as a function of the draw ratio. The good agreement between the experimental values (continuous line) and the theoretical values calculated from Equation 7 (solid points) is also illustrated.

Values of  $n_a^{\parallel}$ ,  $n_a^{\perp}$  and  $\Delta n_a$  are determined at different draw ratios using Equation 1. Fig. 6 shows the variations of the mean refractive index of vestan fibres for plane polarized light vibrating parallel and perpendicular to the fibre axis by increasing the draw ratio. Fig. 7 shows birefringence  $\Delta n_a$  of vestan fibre at different draw ratios.

TABLE I Values of Poisson's ratio of vestan fibres over different draw ratios (temperature of  $33.5^\circ\text{C}$ )

$R$	$\Delta A$ ( $\mu\text{m}^2$ )	$\Delta r$ ( $\mu\text{m}$ )	$A$ ( $\mu\text{m}^2$ )	$r$ ( $\mu\text{m}$ )	$\mu$
1.000	0	0	$1.36 \times 10^3$	20.83	—
1.024	32.0	0.245	$1.33 \times 10^3$	20.59	0.490
1.048	62.5	0.479	$1.30 \times 10^3$	20.36	0.479
1.072	91.7	0.702	$1.27 \times 10^3$	20.13	0.468
1.096	119.6	0.916	$1.24 \times 10^3$	19.92	0.458
1.120	146.2	1.120	$1.21 \times 10^3$	19.72	0.448

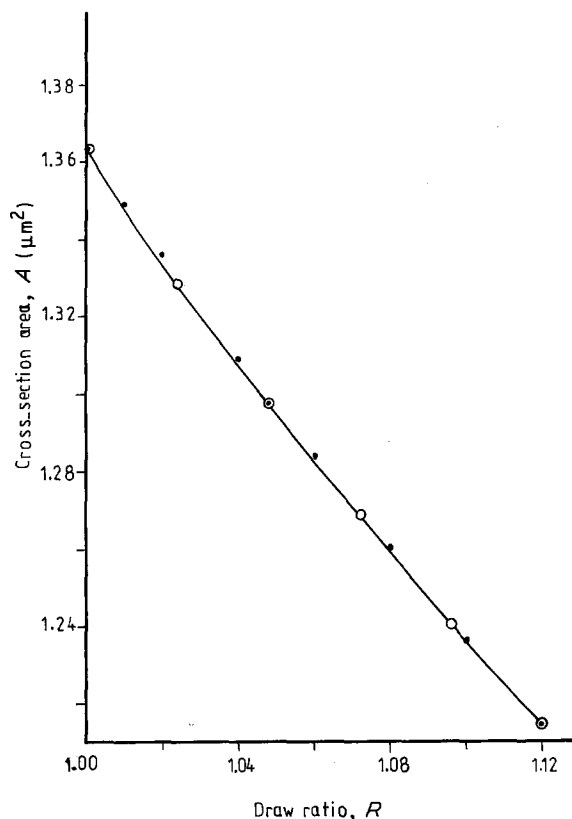


Figure 5 Relation between the mean cross-sectional area of vestan fibres as a function of draw ratio, the continuous curve is estimated from the measurements, while the full points are calculated from Equation 7.

A plot of strain  $\varepsilon = \Delta l/l$  against the birefringence  $\Delta n_a$  of vestan fibre gives a straight line whose equation could be in the following form

$$\Delta n = p + c_e \varepsilon \quad (9)$$

where  $p$  is a constant equal to 0.1006,  $c_e$  the strain optical coefficient [12] and

$$c_e = d(\Delta n)/d\varepsilon = 0.1$$

Table II contains the calculated values of the polarizabilities per unit volume of vestan fibres  $P_a^{\parallel}$ ,  $P_a^{\perp}$  and  $\Delta P_a$  as calculated from Equation 2.

The development of the stress-strain device enables us to determine Young's modulus,  $E$ , of the fibre under test as well as some other associated elastic moduli [16]. Table III contains experimental values of Young's modulus,  $E$ , at different draw ratios as calculated using Equation 3. The elastic shear modulus

$$G = E/2(1 + \mu) \quad (10)$$

TABLE II Calculated values of polarizabilities per unit volume of vestan fibres at different draw ratios

R	$P^{\parallel}$	$P^{\perp}$	$\Delta P$
1.000	0.0859	0.0747	0.0112
1.024	0.0860	0.0746	0.0115
1.028	0.0861	0.0745	0.0115
1.048	0.0861	0.0744	0.0117
1.056	0.0862	0.0744	0.0118
1.072	0.0863	0.0743	0.0120
1.085	0.0863	0.0742	0.0122
1.096	0.0864	0.0741	0.0123
1.113	0.0865	0.0740	0.0125
1.120	0.0865	0.0740	0.0125

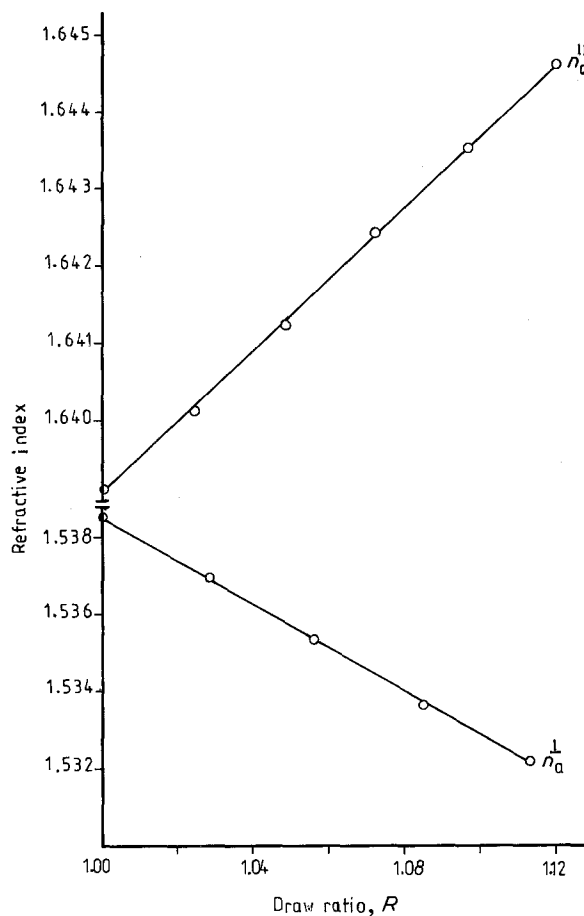


Figure 6 The relation between  $n_a^{\parallel}$  and  $n_a^{\perp}$  as a function of the draw ratio.

and the compressability

$$\chi = 3(1 - 2\mu)/E \quad (11)$$

could also be determined ( $\mu =$  Poisson's ratio).

Fig. 8 shows the variation of different elastic moduli and birefringence of vestan fibres due to different draw ratios.

### 3. Discussion and conclusion

One of the most common methods of changing the structure of a polymeric material to strengthen it, is by drawing it during processing. This orients its chains and supermolecular structures. If the polymer is amorphous with molecules of regular structure, it may even crystallize [17].

Most synthetic fibres are drawn to several times their extruded length to give satisfactory properties. During this process the final crystalline structure is established. In some materials the undrawn fibre is non-crystalline, and the drawing promotes orientation of the molecules is followed by crystallization [18]. Thus a distinction can be made between undrawn and

TABLE III Values of Young's modulus of vestan fibres at different stresses (temperature of 33.5°C)

m (kg)	A (m <sup>2</sup> )	Stress (Pa)	Strain	E (GPa)
0	$1.36 \times 10^{-9}$	0	0	—
$4.0 \times 10^{-3}$	$1.33 \times 10^{-9}$	$28.79 \times 10^6$	0.024	1.12
$6.8 \times 10^{-3}$	$1.30 \times 10^{-9}$	$50.23 \times 10^6$	0.048	1.05
$9.3 \times 10^{-3}$	$1.27 \times 10^{-9}$	$70.34 \times 10^6$	0.072	0.98
$11.5 \times 10^{-3}$	$1.24 \times 10^{-9}$	$88.97 \times 10^6$	0.096	0.93
$13.7 \times 10^{-3}$	$1.21 \times 10^{-9}$	$108.38 \times 10^6$	0.120	0.90

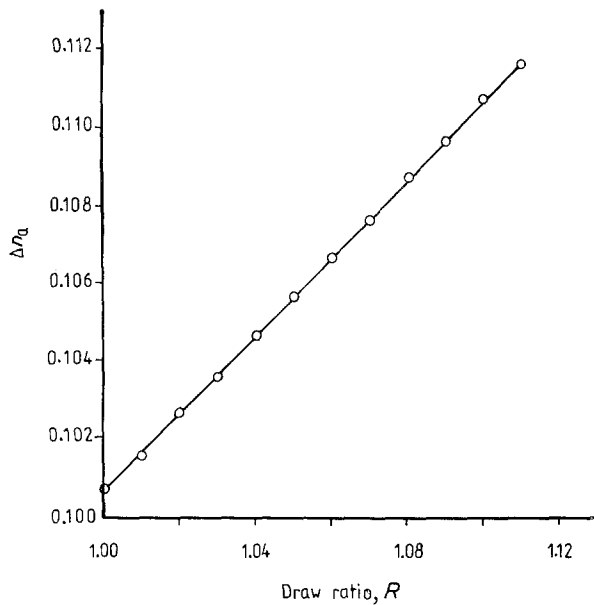


Figure 7 Relation between the mean birefringence  $\Delta n_a$  of vestan fibres and the draw ratio.

drawn synthetic fibres. The values for the birefringence of these fibres have proven to be useful in the adjustment of the drawing process [11].

The present work greatly strengthens the idea that the application of multiple-beam Fizeau fringes is suitable to determine many important optomechanical properties. A knowledge of these mechanical variations with optical parameters is very valuable for characterizing the optomechanical properties of fibres by one technique.

In conclusion, it is clear that the multiple-beam Fizeau fringes technique is useful to clarify the mechanism of the optical behaviour of vestan fibres with different draw ratios. From the measurements carried out for vestan fibres, the following conclusions may be drawn.

(1) The direction dependence of the refractive index was cited by early workers as a proof of the presence of crystalline elements within a fibre. As  $n_a^{\parallel}$  and  $P_a^{\parallel}$

increase with different draw ratios this means increased crystallinity of the fibre.

(2) As the draw ratio increases the double refraction and  $\Delta P_a$  increase. This means that the inherent optical anisotropy of the chain-like macromolecules from the preferred axial orientation of the molecular chains that constitute the fibre, increases.

(3) The microinterferograms clearly identify differences in optical path variations due to undrawn and drawn fibres.

(4) The dimensional changes of the fibres is a function of draw ratio.

(5) Two empirical formulae are suggested to relate (a) the variation of the cross-section area of vestan fibres with the draw ratio and (b) the variation of strain with the birefringence.

(6) As the draw ratio increases,  $\Delta n_a$  increases accompanied by variations of the mechanical parameters. Poisson's ratio, the elastic shear modulus and Young's modulus are decreased by the drawing effect while compressibility is increased.

(7) This modified stress-strain device gives good dynamical behaviour of the optical parameters related with the mechanical properties of the fibre. All measurements are carried out on fibres under equilibrium between the external applied force and the internal molecular attraction force.

(8) Drawing the fibrous structure, however slightly affects the transport properties.

We conclude from the above results and considerations that the practical importance of these measurements provides acceptable results for the optomechanical parameters. Since  $\Delta n$  and  $\Delta P$  are a consequence of the material stretched, so orientational strengthening of polymers may occur not only during fabrication but also during deformation and drawing. The present simply designed microstress-strain device used to study the orientation of fibres would enable fibre producers also to study the different optomechanical properties. This is done under varying conditions for relatively high birefringence fibres.

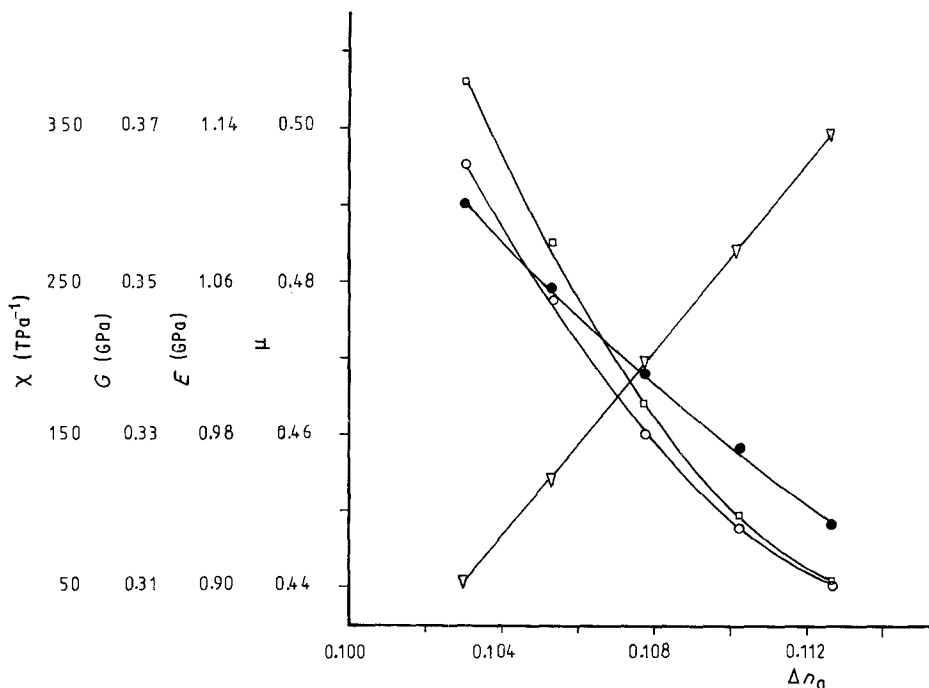


Figure 8 Relation between elastic moduli of vestan fibres and the birefringence  $\Delta n$ . ( $\square$   $G$ ,  $\circ$   $E$ ,  $\bullet$   $\mu$ ,  $\nabla$   $\chi$ ).

## References

1. A. E. ZACHARIADES and R. S. PORTER, in "The Strength and Stiffness of Polymers" (Marcel Dekker, New York, 1983) p. 20.
2. R. H. PETER, "Textile Chemistry", Vol. 1 (Els Pub. Co., London, 1963) p. 396.
3. N. BARAKAT and H. A. EL-HENNAWI, *Tex. Res. J.* **41** (1971) 391.
4. M. PLUTA, *J. Microsc.* **96** (1972) 309.
5. A. A. HAMZA, *ibid.* **142** (1986) 35.
6. I. M. FOU DA, M. M. EL-NICKLAWY, T. EL-DESSOUKI and K. A. EL-FARAHATY, *Acta Phys. Polon.* **A69** (1986) 629.
7. I. M. FOU DA, M. M. EL-NICKLAWY, K. A. EL-FARAHATY and T. EL-DESSOUKI, *J. Text. Inst.* **5** (1987) 378.
8. P. R. BLAKEY, D. E. MONTGOMERY and H. M. SUMNER, *ibid.* **61** (1970) 234.
9. A. UTSUO and R. S. STEIN, *J. Polym. Sci.* **5** (1967) 583.
10. A. R. KALYANARAMAN and R. RAMAKRISHNAN, *J. Text. Inst.* **69** (1978) 351.
11. H. de VRIES, *J. Polym. Sci.* **34** (1959) 761.
12. H. ANGAD GAUR and H. de VRIES, *ibid.* **13** (1975) 835.
13. I. M. FOU DA and K. A. EL-FARAHATY, *Mansoura Sci. Bul.* **13** (1986) 639.
14. A. A. HAMZA and M. KABEEL, *J. Phys. D* **20** (1987) 963.
15. A. A. HAMZA, I. M. FOU DA, K. A. EL-FARAHATY and S. A. HELALY, *Polymer Testing* **7** (1987) 329.
16. D. MENDE and G. SIMON, "Physik: Gleichungen und Tabellen" (VEB Fachbuchverlag, Leipzig, GDR, 1983) pp. 56-60.
17. T. TAGER, "Physical Chemistry of Polymer" (Mir Pub, 1978) p. 245.
18. J. W. S. HEARLE, *J. Appl. Polym. Sci.* **7** (1963) 1193.

*Received 29 September 1988  
and accepted 13 February 1989*